Full length article

An albumin-angiotensin converting enzyme 2-based SARS-CoV-2 decoy with FcRn-driven half-life extension

Elisabeth Fuchs[a], Imke Rudnik-Jansen[a], Anders Dinesen[a], Denis Selnihhin[b], Ole Aalund Mandrup[a], Kader Thiam[c], Jørgen Kjems[a], Finn Skou Pedersen[b], Kenneth A. Howard[a,*]

[a] Interdisciplinary Nanoscience Center (iNANO), Department of Molecular Biology and Genetics, Aarhus University, 8000 Aarhus C, Denmark
[b] Department of Molecular Biology and Genetics, Aarhus University, 8000 Aarhus C, Denmark
[c] GenOway, Lyon 69362 CEDEX 07, France

ABSTRACT

The emergence of new severe acute respiratory syndrome coronavirus 2 (SARS-CoV-2) mutants and breakthrough infections despite available coronavirus disease 2019 (COVID-19) vaccines calls for antiviral therapeutics. The application of soluble angiotensin converting enzyme 2 (ACE2) as a SARS-CoV-2 decoy that reduces cell bound ACE2-mediated virus entry is limited by a short plasma half-life. This work presents a recombinant human albumin ACE2 genetic fusion (rHA-ACE2) to increase the plasma half-life by an FcRn-driven cellular recycling mechanism, investigated using a wild type (WT) albumin sequence and sequence engineered with null FcRn binding (NB). Binding of rHA-ACE2 fusions to SARS-CoV-2 spike protein subdomain 1 (S1) was demonstrated (WT-ACE2 K_D = 32.8 nM and NB-ACE2 K_D = 31.7 nM) using Bio-Layer Interferometry and dose-dependent *in vitro* inhibition of host cell infection of pseudotyped viruses displaying surface SARS-CoV-2 spike (S) protein. FcRn-mediated *in vitro* recycling was translated to a five times greater plasma half-life of WT-ACE2 ($t_{1/2}$ β = 13.5 h) than soluble ACE2 ($t_{1/2}$ β = 2.8 h) in humanised FcRn/albumin double transgenic mice. The rHA-ACE2-based SARS-CoV-2 decoy system exhibiting FcRn-driven circulatory half-life extension introduced in this work offers the potential to expand and improve the anti-COVID-19 anti-viral drug armoury.

Statement of significance

The COVID-19 pandemic has highlighted the need for rapid development of efficient antiviral therapeutics to combat SARS-CoV-2 and new mutants to lower morbidity and mortality in severe cases, and for people that are unable to receive a vaccine. Here we report a therapeutic albumin ACE2 fusion protein (rHA-ACE2), that can bind SARS-CoV-2 S protein decorated virus-like particles to inhibit viral infection, and exhibits extended *in vivo* half-life compared to ACE2 alone. Employing ACE2 as a binding decoy for the virus is expected to efficiently inhibit all SARS-CoV-2 mutants as they all rely on binding with endogenous ACE2 for viral cell entry and, therefore, rHA-ACE2 constitutes a versatile addition to the therapeutic arsenal for combatting COVID-19.

1. Introduction

Coronavirus disease 2019 (COVID-19), caused by the severe acute respiratory syndrome coronavirus 2 (SARS-CoV-2) first identified in December 2019, has become a global pandemic [1]. As of February 2022, more than 424 million cases of COVID-19, including 5.89 million deaths have been reported worldwide [2]. Several COVID-19 vaccines based on mRNA [3], viral DNA [4,5], inactivated virus [6] and protein subunits [7] are included in national vaccination programmes. The vaccines, however, are not accessible for all, and can be ineffective in patients undergoing immunosuppressive treatments [8,9]. Furthermore, adverse side-effects can be associated with the vaccines such as anaphylaxis or myocarditis with lipid-based mRNA-based COVID-19 vaccines [10], and thrombosis and thrombocytopenia syndrome with adenoviral

vector-based COVID-19 vaccines [11]. Moreover, emergence of new SARS-CoV-2 mutants may require seasonal vaccine redesign. The World Health Organization (WHO) classifies five SARS-CoV-2 variants (Alpha, Beta, Gamma, Delta and Omicron) for concern, with four shown to influence vaccine efficacy. In particular, significantly reduced neutralising antibodies are associated with the Delta and Omicron variants [12–14]. This highlights the need for new effective anti-viral therapeutics that can combat arising virus mutants.

SARS-CoV-2 enters cells by interaction of the receptor binding domain (RBD) in viral transmembrane spike (S) protein with cell membrane bound carboxypeptidase angiotensin converting enzyme 2 (ACE2) [15]. Recombinant human ACE2 (rhACE2) ectodomain, that resembles the endogenous viral cell entry receptor, has been used as a COVID-19 decoy and completed Phase I and II clinical trials, showing significant reduction in time on mechanical ventilation [16–18]. Furthermore, the therapeutic efficacy may also be enhanced through the negative regulator/modulator function of ACE2 on the peptide hormone angiotensin (Ang) II that is associated with acute lung injury linked to the severity of COVID-19 [18,19]. ACE2 can counterbalance Ang II functions by cleaving Ang II into Ang 1-7 and, thereby, counteract Ang II overactivity [18,20]. The duration of rhACE2 efficacy, however, is limited by a plasma half-life of ∼10 h in humans [16].

Genetic fusion of rhACE2 to an immunoglobulin Fc region that interacts with the cellular recycling neonatal Fc receptor (FcRn) has been utilised as a strategy to extend the blood residence time of rhACE2 [21–23]. Induction of cytokine release syndrome (CRS), however, can result from high-level immune activation mediated by Fc interaction with Fcγ receptors (FcγRs) on immune cells [24]. This potentially life-threatening cytokine release can lead to cardiac dysfunction, respiratory distress syndrome and renal and/or hepatic failure [25]. Antibody-dependent enhancement (ADE) of virus infection is another mechanism by which the virus can infect host cell [26]. Virus-antibody immune complexes have shown to bind FcγRs that can be internalised, leading to enhanced entry of the virus into host cells. The risk of exacerbating COVID-19 severity through FcγR engagement of virus-antibody complexes is a limitation for antibody-based drug designs [26]. Human serum albumin (HSA) does not engage with the classical FcγRs [27] but with the non-classical FcγRs, such as FcRn, to facilitate a long plasma half-life of approximately 19 days [27,28] that has been adopted in marketed albumin-based drugs [29,30]. Furthermore, single-point amino acid substitutions in HSA domain III have been used to tune the affinity to FcRn [31]. In this work, we designed recombinant human albumin-ACE2 (rHA-ACE2) fusions incorporating albumin sequences engineered with wild type (WT) or null-binding (NB) FcRn binding affinity in order to investigate the mechanistic role of FcRn-mediated cellular recycling in plasma half-life extension for potential exploitation in COVID-19 therapies.

2. Materials and methods

2.1. cDNA design, construction and production of expression vectors

The rHA-ACE fusion proteins were designed by codon optimizing the nucleic acid sequence of the ACE2 ectodomain (amino acids 18-740 of Uniprot ID: Q9BYF1-1) for expression in a human cell line. This was subcloned by GenScript into pcDNA3.1 plasmids containing the WT and KAHQ (NB) variants [32]. Nucleic acids encoding a single GGGGS peptide linker connects the ACE2 C-terminal and the rHA N-terminal.

Plasmids were amplified by transformation into TOP10 chemically competent *E. coli* using heat shock (40 min on ice, 2 min at 42 °C, 5 min on ice) and plated on agar plates (1% peptone (Merck, #82303), 0.5% yeast extract (Fisher Scientific, #BP9727), 0.8% NaCl (Acros Organics, #207790010), 1.5% agar (Sigma, #05040), and

0.1 mg/mL ampicillin (Fisher Scientific, #BP1760)) and cultured overnight. A single colony was selected and grown overnight in a peptone yeast extract broth (3.2% peptone, 2% yeast extract, and 0.5% NaCl) under selection with 0.1 mg/mL ampicillin (Fisher Scientific, #BB176-25). Plasmids were purified using the NucleoBond Xtra Maxi (Macherey-Nagel, #740414) according to the manufacturer's protocol.

2.2. Protein expression and purification

The rHA-ACE2 fusions were transiently expressed in HEK293E cells cultured under standard conditions; 37 °C, 5% CO$_2$ in serum-free Freestyle^{TM} 293 expression media (Gibco, #12338018). Polyethylenimine (transfection grade linear PEI MW 40kDa, PolySciences, #24765-1) and plasmid DNA were separately diluted in Optimem (Gibco, #11058-021), mixed in a 4:1 mass ratio and incubated for 15 min before mixing with FreeStyle 293 expression medium and added to 55–65% confluent HEK293E cells in 5-layer bottles (Corning, #353144). Complete protease inhibitor (Roche, #11873580001) was added to the conditioned medium and centrifuged (300 g, 10 min) before sterile filtering (Corning, #431098) and storage at 4 °C. Protein was harvested from supernatant and purified using a CaptureSelect human albumin affinity matrix (Thermo Fisher, cat#191297005) by elution with 2 M MgCl$_2$ at pH 7.4. Concentration and buffer exchange into phosphate buffered saline (PBS) of the purified protein was performed using VivaSpin2 centrifugal concentrators (Sartorius, #VS0231). Subsequently, purified protein was snap frozen in liquid N$_2$ and stored at -140 °C.

2.3. SDS-PAGE and Western blot analysis

Protein samples were separated on 10% SDS-PAGE and visualised by Coomassie Blue staining or blotted onto a PVDF membrane (Novex, #LC2005) for Western blot analysis. Membranes were blocked in 2% w/v skimmed milk powder in PBS (mPBS) and incubated for 2 h at room temperature (RT). For Western blot analysis of albumin, membranes were incubated with horseradish peroxidase (HRP) conjugated polyclonal goat anti-HSA antibody (Abcam, #ab19183) diluted 1:2000 in 2% mPBS for 2 h at RT and subsequently washed 3 times in PBS before detection with TMB substrate (Sigma, #T0565). For Western blot analysis of ACE2, membranes were first incubated with monoclonal mouse anti-human ACE2 antibody (RnD System, #MAB933) diluted 1:250 in mPBS for 2 h at RT and washed 3 times in PBS before incubation with polyclonal HRP conjugated goat anti-mouse immunoglobulins antibody (Dako Agilent, #P0477) diluted 1:500 in mPBS for 2 h. Membranes were subsequently washed 3 times in PBS before developing with TMB substrate.

2.4. rHA-ACE2 fusion binding to SARS-CoV-2 S1 using Bio-Layer Interferometry

Binding kinetics of rHA-ACE2 to biotinylated SARS-CoV-2 S1 protein (Acro Biosystems, #S1N-C82E8) was measured by Bio-Layer Interferometry (BLI) using an Octet Red 96e system (Sartorius). Soluble ACE2 (Sigma Aldrich, #SAE0064) was used as a control. The biotinylated SARS-CoV-2 S1 protein was immobilised on Streptavidin Dip and Read^{TM} sensor tips at a concentration of 8 nM in kinetics buffer (PBS supplemented with 0.02% Tween-20 and 0.1% bovine serum albumin (BSA)). For binding kinetics measurements rHA-ACE2 and soluble ACE2 samples were prepared in a 7-step two-fold dilution series starting at 3 μM and 125 nM, respectively, in kinetics buffer. Measurements were performed at 30 °C and 1000 rpm shaking with a 200 s association and 600 s dissociation step. Tips were regenerated between samples by alternating

between 10 s incubation in 10 mM Glycine at pH 3 and kinetics buffer 6 times. SARS-CoV-2 S1 protein coated streptavidin sensors in kinetics buffer was used for baseline subtraction. Data analysis was performed using the Octet data analysis software (version 10.0.1.6) using a 1:1 interaction model curve fitting.

2.5. Virus-like particles inhibition assay

The inhibitory effect of the rHA-ACE2 fusion on viral cell entry was investigated using virus-like particles (VLPs) decorated with SARS-CoV-2 S protein, as previously described [33]. In brief, HEK293T cells were transfected with lentiviral packaging vectors encoding the gag-pol, REV and eGFP reporter gene (a gift from Prof. Jacob Giehm Mikkelsen, Aarhus University, Denmark) and a SARS-CoV-2 S protein plasmid (a gift from Zhaohui Qian, Addgene plasmid, #145780) at a ratio of 3:6:4:4 by calcium phosphate precipitation. Media was exchanged after 24 h and VLPs were harvested from the cells 48 h post transfection, filtered (0.45 µm), and incubated with rHA-ACE2 fusion, soluble ACE2 or PBS as a control for 1.5 h at 37 °C and 5% CO_2. The pre-incubated VLPs were subsequently transferred to HEK293T cells, previously transfected with TMPRSS2 (a gift from Roger Reeves, Addgene plasmid #53887) and human ACE2 (a gift from Hyeryuen Cho, Addgene plasmid #1736) by calcium phosphate precipitation, seeded at a density of 10,000 cells/well at a 1:1 ratio. The media was exchanged after 24 h, and cells were further cultured for 72 h. Transduced cells were analysed for eGFP fluorescence by fluorescence microscopy (IX73 inverted microscope, Olympus equipped with DP73 camera, Olympus) and flow cytometry (Cytoflex, Beckman Coulter) and analysed using the CytExpert software. The infectivity of VLPs pre-incubated with rHA-ACE2 fusions or soluble ACE2 was normalized to the infectivity of VLPs pre-incubated with PBS. IC_{50} values were determined using the Origin 2018 software.

2.6. Cellular recycling of rHA-ACE2 in HMEC-1-FcRn cells

Human dermal microvascular endothelial cells (HMEC-1) stably overexpressing human FcRn (HMEC-1-FcRn) were cultured in complete media consisting of MCDB 131 (Gibco, #61965026) supplemented with 10 ng/mL recombinant human epidermal growth factor (rhEGF, Peprotech, #0617AFC05), 1 µg/mL hydrocortisone (Sigma Aldrich, #H088), 50 µg/mL G418 (Sigma Aldrich, #2241417), 0.25 µg/mL Puromycin (Life Technologies, #1894263), 2 mM L-glutamine (Lonza, #BE17-605E) and 10% FBS.

The cellular recycling assay was performed as previously described [28]. In brief, HMEC-1-FcRn cells, stably overexpressing human FcRn, were seeded at a density of 1×10^5 cells per well in 48 well plates coated with 1:50 dilution of Geltrex (Gibco, #2248603) in PBS. When near confluent, cells were washed twice with preheated PBS and incubated for 1 h at 37 °C and 5% CO_2 with 0.15 µM of rHA-ACE2 fusions or rHA controls in Hank's buffered salt solution (HBSS) adjusted to pH 6 with 1 M 2-(N-morpholino)ethanesulfonic acid (MES) buffer. Cells were subsequently washed 5 times with ice cold PBS and left for 1 h at 37 °C and 5% CO_2 in 160 µL/well release media (complete media without FBS). Supernatant was harvested and analysed by sandwich ELISA.

For the sandwich ELISA analysis of the supernatants, Maxisorp plates (Thermo Fisher, #442404) were coated for 2 h at RT with polyclonal goat anti-HSA antibody (Sigma Aldrich, #A-7544), diluted 1:1000 in PBS. Coated plates were then blocked with 2% mPBS for 2 h at RT followed by washing three times with PBS supplemented with 0.05% Tween (PBST). Supernatant samples and albumin controls were added to the plates and incubated

overnight at 4 °C. For detection, plates were incubated for 1 h at RT with polyclonal HRP conjugated goat anti-HSA antibody (Abcam, # ab19183) followed by washing three times with PBST and developing with TMB PLUS2 substrate (Kem-En-Tec Diagnostics, #4395). All samples were performed in quadruplicates and the experiment was repeated five times.

2.7. Animals

Female and male double transgenic human FcRn ($hFcRn^{+/+}$)/human serum albumin ($hAlb^{+/+}$) with a C57BL/6 background [34] were supplied by GenOway (Lyon, France). Pharmacokinetic studies were performed at the Animal Facility, Department of Biomedicine, Aarhus University, in accordance with the ethical approval in national guidelines for care and use of laboratory animals under the Danish Animal Experiment Inspector license #2018-15-0201-01399. Animals were housed in polycarbonate cages with wire tops, wood chip bedding, and access to *ad libitum* food and tap water.

2.8. Circulatory half-life of rHA-ACE2 fusions

Male and female mice were randomly divided into the following experimental groups; WT-ACE2 ($N = 4$), NB-ACE2 ($N = 5$) and soluble ACE2 ($N = 6$). Three male mice were used for a PBS control. Mice were intravenously injected in the tail vein with either 4 mg/kg rHA-ACE2 fusion or an equimolar concentration of 2.3 mg/kg soluble ACE2 or PBS. Blood samples were collected from the tip of the tail vein in 20 µL heparinized microcapillary tubes 1 min, 4 h, 8 h, 24 h, 48 h, 72 h, 144 h, 216 h, 312 h and 384 h post injection. Collected blood was diluted 1:10 in PBS, spun down to collect serum supernatant and frozen at -20 °C until analysis by sandwich ELISA.

For serum detection by sandwich ELISA, Maxisorp plates (Thermo Fisher, #442404) were coated with capture antibodies (rHA-ACE2: monoclonal mouse anti-human ACE2 (RnD Systems, #MAB933) diluted 1:500 and for ACE2: goat anti-ACE2 (Abcam, #AF933) diluted 1:500) in PBS for 2 h at RT. Plates were first washed once with PBST and three times with PBS. Plates were then blocked with 2% mPBS for 2 h at RT and subsequently washed once in PBST and three times in PBS. Mouse serum samples or rHA-ACE2 standard series were then added and incubated overnight at 4 °C. Plates were washed once in PBST and three times in PBS before incubation with detection antibodies conjugated with HRP (rHA-ACE2: polyclonal goat anti-HSA (Abcam, #ab19183) diluted 1:10,000 and ACE2: monoclonal anti-poly Histidine-Peroxidase (Sigma-Aldrich, #A7058-1VL) in 2% mPBS for 2 h at RT. After washing once with PBST and three times with PBS, TMB PLUS2 (Kem-En-Tec Diagnostics, #4395) was used for plate development. Data was analysed in GraphPad Prism software version 9.3.1. by a two-phase decay model and interpolation to the associated standard series.

2.9. Statistical analysis

Experimental data was analysed using the Origin 2018 software and GraphPad Prism software v.9. The respective conducted statistical tests are indicated in the corresponding figure and table legends. One-way ANOVA and Turkey's test were used for statistical analysis of BLI experiments and viral inhibition assay. Unpaired t-test was used for statistical analysis of the recycling assay. A minimum value of $p < 0.05$ was considered statistically significant. To ensure reproducibility, all *in vitro* experiments were repeated at least 3 times.
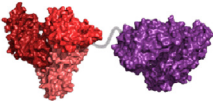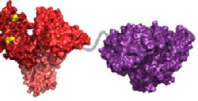
Fig. 1. Design overview of rHA-ACE2 fusions. ACE2 ectodomain (residues 18-740) (purple) was genetically fused to the N-terminus of rHA (red) by a flexible GGGGS linker (grey) and expressed as a single chain protein (150 kDa). Top; Schematic overview of C-terminus to N-terminus. Two different rHA variant sequences, wild-type (WT), and a null-binder (NB) containing point mutations (highlighted in yellow) in albumin domain III resulting in different FcRn affinity, were incorporated in the fusion protein designs.

3. Results

3.1. rHA-ACE2 fusion expression and purification

Recombinant ACE2 ectodomain (residues 18–740) was genetically fused to the N-terminus of rHA WT, or an rHA NB variant engineered for null FcRn engagement by point mutations in the FcRn binding interface (Fig. 1). The fusion proteins expressed in HEK293E cells were purified by HSA affinity chromatography (Supplementary Fig. 1). Identification of rHA-ACE2 fusion protein using SDS-PAGE showed the expected molecular weight of ~150 kDa (Fig. 2A) and albumin (Fig. 2B) and ACE2 components (Fig. 2C) were verified respectively by Western blot analysis.

3.2. Binding of SARS-CoV-2 S1 protein

Binding of rHA-ACE2 to immobilised SARS-CoV-2 S1 protein was investigated by BLI and compared to binding of soluble ACE2 (Fig. 3). Measurements showed high affinity binding of the two rHA-ACE2 fusions (WT-ACE2 and NB-ACE2) (Table 1). The calculated binding kinetics based on a 1:1 fitting model revealed a K_D of 32.8 nM and 31.7 nM for WT-ACE2 and NB-ACE2, respectively,

with no significant differences in binding affinities between the fusions. The K_D of 0.9 nM for soluble ACE2 showed a higher binding affinity compared to rHA-ACE2 fusion proteins, that can be attributed to decreased k_{on} rates of WT-ACE2 (7.86E+03 1/Ms) and NB-ACE2 (9.64E+03 1/Ms) compared to soluble ACE2 (1.84E+05 1/Ms) (Table 1).

3.3. In vitro VLP inhibition

Lentiviral VLPs decorated with the SARS-CoV-2 S protein were used as a model to test *in vitro* viral cell entry inhibition of rHA-ACE2 fusions. HEK293T cells, overexpressing ACE2 and TMPRSS2 required for SARS-CoV-2 cell entry, were used as permissive cell line in combination with an integrated eGFP reporter gene to allow detection of transduced cells (Fig. 4B). Flow cytometric analysis of transduced cells showed efficient dose-dependent inhibition of VLP entry by the rHA-ACE2 fusions and soluble ACE2 (Fig. 4A, Supplementary Fig. 2). The WT-ACE2 and NB-ACE2 fusions exhibited an IC_{50} of 444.0 ± 217.7 nM and 748.0 ± 158.9 nM, respectively, whilst the IC_{50} of soluble ACE2 was 38.5 ± 24.6 nM, that correlated with the binding kinetics observed by BLI. There was no statistically significant difference observed between the IC_{50} values of the two rHA-ACE2 fusions (WT-ACE2 and NB-ACE2). Control WT rHA did not show any inhibitory effect on the VLPs at any of the investigated concentrations.

3.4. FcRn-mediated cellular recycling

A cellular recycling assay established by our group [28,35] was utilised to investigate FcRn-mediated cellular recycling of rHA-ACE2 in HMEC-1-FcRn overexpressing cells. Different rHA standard variants with engineered FcRn affinities, referred to as NB rHA and WT rHA, were used to validate the assay (Fig. 5). The level of recycled protein in the media was determined by sandwich ELISA detecting the rHA component of the rHA-ACE2 fusions. The cellular recycling showed the expected difference of WT-ACE2>NB-ACE2, that was greater than the cellular recycling detected for WT rHA (Fig. 5).

3.5. In vivo circulatory half-life of rHA-ACE2 fusions

The circulatory half-life of rHA-ACE2 fusions were benchmarked against soluble ACE2 in the double transgenic mouse model with both human FcRn and HSA genes (hFcRn+/+, hAlb+/+) under the control of an endogenous promoter [34]. Proteins were intravenously administered by tail vein injection, and blood subsequently collected at selected time points to determine intact full-size protein levels in serum by sandwich ELISA. The circulatory half-life calculated from the elimination phase ($t_{1/2}$ β) was shown
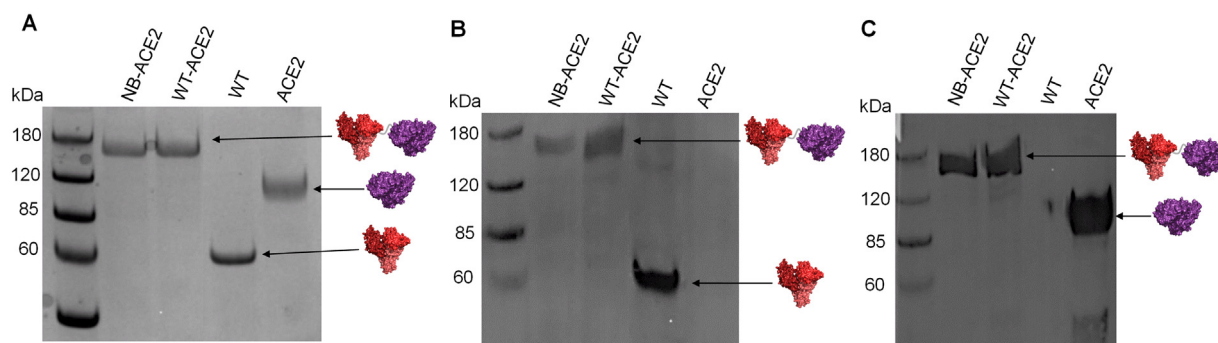

Fig. 2. SDS-PAGE and Western blot analysis of purified rHA-ACE2 fusion protein. (A) Coomassie blue stained SDS-PAGE of the two constructs NB-ACE2 and WT-ACE2 (150 kDa). In addition, WT rHA (66.5 kDa) and soluble ACE2 (85.9 kDa) were used as controls. (B) Western blot detection of rHA in NB-ACE2 and WT-ACE2. ACE2 and WT rHA were included as controls. (C) Western blot detection of ACE2 in NB-ACE2 and WT-ACE2.WT rHA and ACE2 were included as controls.
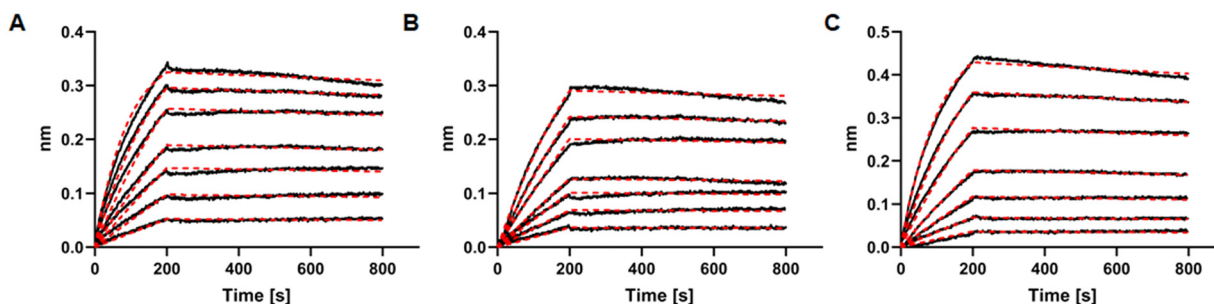
Fig. 3. Binding kinetics measurements. Sensorgrams showing binding of (A) WT-ACE2, (B) NB-ACE2, and (C) ACE2 to immobilised SARS-CoV-2 S1 protein. Binding of rHA-ACE2 fusions was investigated using a 2-fold dilution series from 3 μM to 0.046 μM and for ACE2 from 125 nm to 1.9 nM. Raw data is depicted in black and data fitted to a 1:1 model in red. $N = 3$ independent experiments.

Table 1
Measured binding kinetics parameter of rHA-ACE2 fusions and soluble ACE2 interaction with SARS-CoV-2 S1. Binding affinities were determined by a 1:1 fitting model. Statistical significance was evaluated using One-Way ANOVA and Turkey's test in Origin 2018 software, $N = 3$ independent experiments.

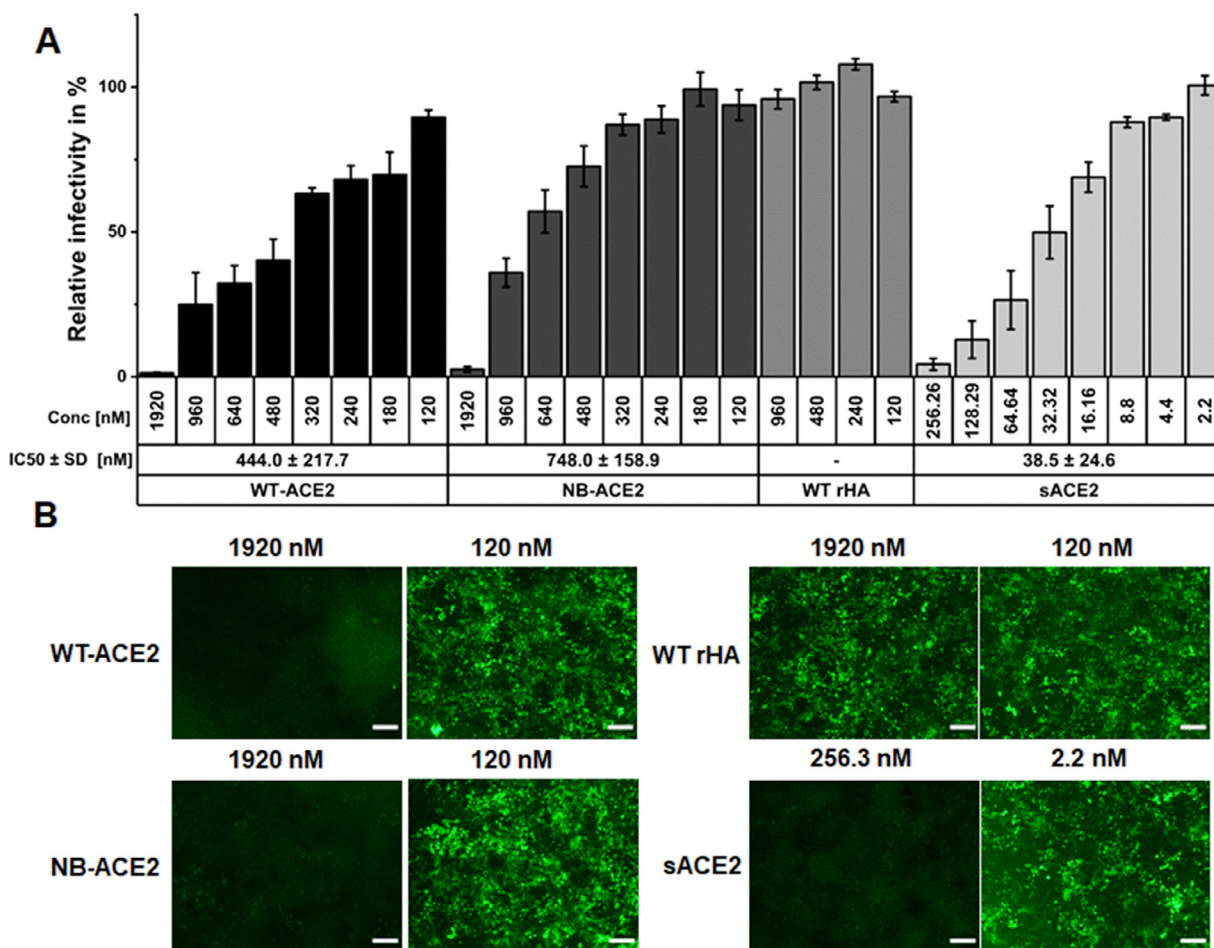|	K_D (SD) [M]	k_{on} (SD) [1/Ms]	k_{off} (SD) [1/s]	X^2	R^2
WT-ACE2	3.28E-08 (± 9.569E-09)	7.86E+03 (± 4.420E+03)	2.80E-04 (± 1.953E-04)	0.203	0.9961
NB-ACE2	3.17E-08 (± 1.926E-08)	9.64E+03 (± 7.535E+03)	2.09E-04 (± 1.324E-04)	0.085	0.998
ACE2	8.84E-10 (± 5.353E-10)	1.84E+05 (± 1.00E+05)	1.27E-04 (± 0.22E-04)	0.103	0.996

Fig. 4. *In vitro* VLP inhibition assay. (A) Flow cytometry analysis of the relative infectivity of VLPs, displaying the SARS-CoV-2 S protein, incubated with rHA-ACE2 fusions (WT-ACE2 and NB-ACE2), WT rHA or soluble ACE2 (sACE2) at different concentrations, compared to VLPs incubated with equivalent volume of PBS. $N = 3$ independent experiments, error bars indicate standard error of mean (SEM). Mean IC$_{50}$ and SD of WT-ACE2, NB-ACE2, and sACE2 obtained from dose response fit of viral inhibition assay data is included. Statistical significance was evaluated using One-Way ANOVA and Turkey's test in Origin 2018 software. (B) Representative Fluorescence Microscopy images of HEK293-T cells incubated with VLPs with surface SARS-CoV-2 S protein and rHA-ACE2 fusions (WT-ACE2 and NB-ACE2), WT rHA and sACE2 at different concentrations. Each image has a size of 1.8 mm x 1.3 mm with scalebars indicating 200 μm. Transduced cells express eGFP, untreated cells and cells treated with VLPs and PBS were used as negative and positive control, respectively.
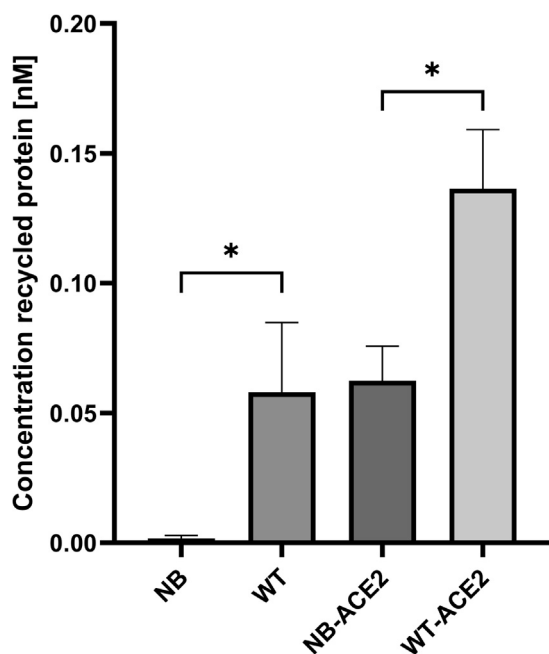
Fig. 5. FcRn-mediated cellular recycling of rHA-ACE2 fusions. Recycled levels of NB-ACE2 and WT-ACE2, and NB rHA and WT rHA variants in HMEC-1-FcRn cells. Unpaired t-test statistics using GraphPad prism software v.9 with, $*p < 0.05$, $N = 5$ independent experiments, error bars indicate SEM.

to be 13.5 h and ~3.1 h for WT-ACE2 and NB-ACE2 fusions, respectively, compared to the $t_{\frac{1}{2}}$ β of approximately 2.8 h for soluble ACE2 (Fig. 6).

4. Discussion

One of the first compounds investigated for treatment of COVID-19 was soluble rhACE2, used to neutralise SARS-CoV-2 and minimise organ injury related to increased Ang II concentrations [18]. The potential of rhACE2 as a decoy for SARS-CoV-2 by mimicking its cognate cell entry receptor is exemplified in a recent phase II clinical trial and case study [17,18]. Fusion of the rhACE2 protein to an immunoglobulin Fc region has led to improved circulatory half-life of the decoy due to FcRn-mediated cellular recycling of the protein *in vivo* [21–23]. In recent work, the humanised decoy antibody ACE2-Fc fusion protein abrogated virus replication in ACE2-expressing lung cells and lung organoids [36]. In another study, recombinant ACE2-IgG1 Fc or ACE2-IgA Fc fusion proteins incorporated an ACE2 sequence optimised for enhanced binding affinity to S protein of different virus variants [37]. A rhACE2-Fc fusion protein has also been investigated in a transgenic hACE2 mouse model and showed dose-dependent prophylactic and therapeutic efficacy compared to soluble ACE2 [38]. Interaction of the Fc fragment with FcγRs on immune cells, however, can potentially elicit adverse effects by exaggerating an adverse immune response in COVID-19 [39]. In this work, we adopted albumin as an alternative half-life extension technology to overcome the risks associated with Fc fusions. An rHA-ACE2 fusion containing a wild type albumin sequence, and an FcRn null-binding albumin sequence [32], previously shown by our laboratory to provide a tool to investigate mechanistic FcRn-driven cellular recycling of an alternative albumin fusion [40], were produced. Inclusion of an NB-ACE2 variant allowed investigations into the influence of the fusion on the engagement of rHA with FcRn and confirmation of a predominant FcRn-driven half-life extension rather than a molecular weight effect.

The mechanism by which SARS-CoV-2 infects host cells is dependent on the virus transmembrane S protein targeting membrane bound ACE2 [41], therefore, complex formation between the viral S protein and designed ACE2 decoy is crucial. BLI analysis of rHA-ACE2 binding affinity to SARS-CoV-2 S1 protein showed the equilibrium dissociation constant to be in the nanomolar range, but with lower affinity compared to soluble ACE2. The reduced binding affinities of rHA-ACE2 fusions most likely arise from fusing the ACE2 ectodomain to albumin, which may cause some steric hindrance on binding. The binding affinities, however, are still similar to ACE2-Fc fragment fusions previously reported in preclinical studies [21,23]. The rHA-ACE2 fusions were able to prevent VLP infection of host cells, even though the IC_{50} values were increased compared to soluble ACE2, possibly due to steric hindrance effects on VLP engagement from incorporation of albumin. Optimisation of the linker flexibility and length between the rHA and ACE2 domain in the fusion could potentially reduce steric hindrance and increase the inhibitory effect of the fusion protein. Furthermore, the use of SARS-CoV-2 infection of primary target cells from human airway epithelium or organoids could also be used to further evaluate the natural virus inhibition potential [42]. However, the FcRn-mediated increase in half-life of the fusion protein is expected to more than compensate for the decreased inhibitory efficiency observed *in vitro*.

IC_{50} values, determined by an *in vitro* VLP inhibition assay, between the two fusions were not significantly different, indicating no enhancement in cellular entry due to FcRn engagement. Moreover, this supports ACE2 decoy function not being influenced by amino acid mutations in the predominant FcRn-binding region lying in albumin domain III. Greater cellular recycling of WT-ACE2 was observed in FcRn-overexpressing endothelial cells compared to NB-ACE2 that was included as a negative control to investigate FcRn-driven cellular recycling. This is in accordance with our previous albumin fusion recycling work using the same WT and NB sequence [40]. The concentration of detected protein in medium was increased for the rHA-ACE2 fusion compared to control rHA, possibly due to engagement of the ACE2 domain with other receptors involved in the renin-angiotensin system [43].

The expected FcRn-mediated difference showing WT-ACE2>NB-ACE2 was maintained in a physiologically relevant model, supporting the thesis that the half-life of the fusion protein is highly dependent on FcRn engagement. The WT-ACE2 fusion had a 4.8- ($t_{\frac{1}{2}}$ $\beta = 13.5$ h) and 4.4-fold higher circulatory half-life compared to soluble ACE2 ($t_{\frac{1}{2}}$ $\beta = 2.8$ h) and NB-ACE2 ($t_{\frac{1}{2}}$ $\beta = 3.1$ h), respectively. The circulatory half-life of the rHA-ACE2 fusions were lower than previous studies performed with a bispecific T-cell engager-albumin WT fusion in the same double transgenic (hFcRn$^{+/+}$, hAlb$^{+/+}$) mouse model, where a circulatory half-life of 26 h was obtained [40].

ACE2 is a dipeptidyl carboxypeptidase known to cleave C-terminal dipeptides from angiotensin I to produce angiotensin II [44] and functions similar to carboxypeptidase A (CPA) shown to cleave C-terminal peptides on HSA resulting in reduced FcRn affinity and circulatory half-life [45]. Genetic fusion of ACE2 to the C-terminal of rHA may, therefore, be favourable in future designs. Alternatively, a fusion protein could be designed containing mutations in the ACE2 catalytic active sites that inactivates the enzyme. This approach was applied in previous work by Tada et al. in which the inactivated ACE2 ectodomain fused to Fc domain 3 of the Ig heavy chain could still inhibit viral host cell entry *in vivo* [22]. In addition, serum stability analysis (Supplementary Fig. 3) of the rHA-ACE2 fusion indicated a decline in protein integrity over days in 90% fetal bovine serum. Future work could focus on optimisation of stability parameters such as fusion linker engineering, shown previously to influence the stability of albumin fusion proteins [46]. The substantial increase in circulatory half-life of the
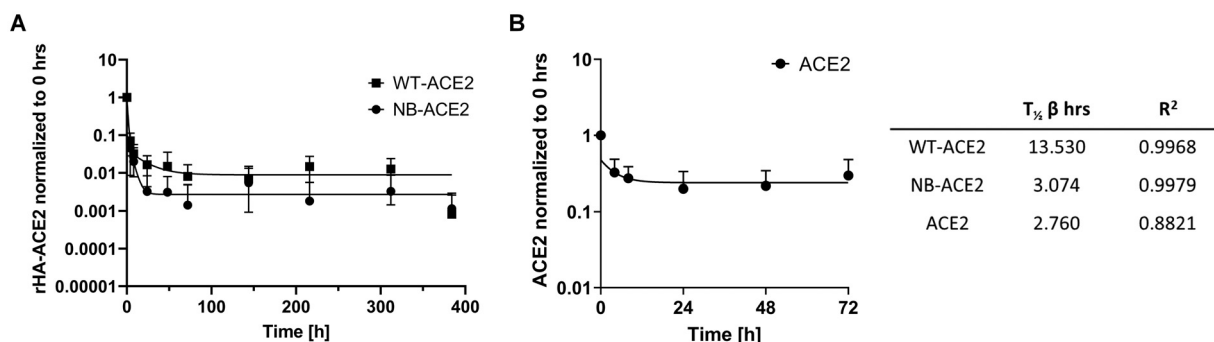
Fig. 6. Circulatory half-life of rHA-ACE2 fusions in hFcRn$^{+/+}$, hAlb$^{+/+}$ mice. (A) rHA-ACE2 (WT and NB) and (B) soluble ACE2 blood samples were drawn at 0 h, 4 h, 8 h, 24 h, 48 h, 72 h, 144 h, 216 h, 312 h and 384 h to detect full size fusion and ACE2 in serum by sandwich ELISA, respectively. The highest concentration in the serum was observed at $t = 0$ hrs and all samples were normalised to the serum concentrations in the 0 h samples. $N = 4$ for WT-ACE2, $N = 5$ for NB-ACE2 and $N = 6$ for ACE2, error bars represent standard deviations. Data was analysed in the GraphPad Prism software v.9 by a two-phase decay model after interpolation to standard series.

WT-ACE2 fusion over soluble ACE2, obtained in our work, is still expected to translate into less frequent dosage and longer lasting effects. However, the therapeutic effect of the fusion protein compared to soluble ACE2 needs to be evaluated in future studies in established COVID-19 models. To better investigate the role of human FcRn-mediated half-life extension on the therapeutic effect, an *in vivo* COVID-19 model with a humanised FcRn and albumin background could be developed. In addition to the therapeutic efficacy, the safety of the fusion protein should be investigated in future work, to evaluate potential adverse effects that may arise from prolonged circulation. However, based on promising clinical trial results on the administration of ACE2 [16,17] and the approval of albumin protein fusions [29,30], minimal side-effects and immunogenicity are anticipated for the rHA-ACE2 fusion protein.

Emergence of new SARS-CoV-2 variants, can potentially decrease the efficacy of current vaccines and antibody treatments [11], and place patients with compromised immune system or other pre-existing medical conditions at higher risk for more severe COVID-19 effects. This highlights the need for a therapeutic, effective against both, existing and future variants of the virus. Potent binding and inhibition of different virus variants has been shown for several ACE2 based decoys [22,37,38], due to the resemblance to the endogenous host cell receptor. The rHA-ACE2 fusion protein, therefore, is also expected to neutralise different mutants with similar potency. The albumin fusion protein may, therefore, provide a valuable tool to effectively treat new emerging SARS-CoV-2 variants. In summary, this work introduces an rHA-ACE2-based SARS-CoV-2 decoy with FcRn-driven half-life extension that can potentially be used to maximise therapeutic effects and expand the required armoury to combat COVID-19.

Data availability

The data supporting the presented findings are provided in the supplementary information. Detailed raw and progressed data can be made available upon reasonable request.

Declaration of Competing Interest

The authors declare that they have no known competing financial interests or personal relationships that could have appeared to influence the work reported in this paper.

Acknowledgments

Supplementary materials

Supplementary material associated with this article can be found, in the online version, at doi:10.1016/j.actbio.2022.09.048.

References

[1] P. Zhou, X.L. Yang, X.G. Wang, B. Hu, L. Zhang, W. Zhang, H.R. Si, Y. Zhu, B. Li, C.L. Huang, H.D. Chen, J. Chen, Y. Luo, H. Guo, R.D. Jiang, M.Q. Liu, Y. Chen, X.R. Shen, X. Wang, X.S. Zheng, K. Zhao, Q.J. Chen, F. Deng, L.L. Liu, B. Yan, F.X. Zhan, Y.Y. Wang, G.F. Xiao, Z.L. Shi, A pneumonia outbreak associated with a new coronavirus of probable bat origin, Nature 579 (7798) (2020) 270–273.

[2] WHO. WHO coronavirus (COVID-19) dashboard. 2022 [cited 2022 23/02]; Available from: https://covid19.who.int/.

[3] E.J. Anderson, N.G. Rouphael, A.T. Widge, L.A. Jackson, P.C. Roberts, M. Makhene, J.D. Chappell, M.R. Denison, L.J. Stevens, A.J. Pruijssers, A.B. McDermott, B. Flach, B.C. Lin, N.A. Doria-Rose, S. O'Dell, S.D. Schmidt, K.S. Corbett, P.A. Swanson 2nd, M. Padilla, K.M. Neuzil, H. Bennett, B. Leav, M. Makowski, J. Albert, K. Cross, V.V. Edara, K. Floyd, M.S. Suthar, D.R. Martinez, R. Baric, W. Buchanan, C.J. Luke, V.K. Phadke, C.A. Rostad, J.E. Ledgerwood, B.S. Graham, J.H. Beigel, R.N.A.S.G. m, Safety and immunogenicity of SARS-CoV-2 mRNA-1273 vaccine in older adults, N. Engl. J. Med. 383 (25) (2020) 2427–2438.

[4] E.H. Livingston, P.N. Malani, C.B. Creech, The Johnson & Johnson vaccine for COVID-19, JAMA 325 (15) (2021) 1575-1575.

[5] M.N. Ramasamy, A.M. Minassian, K.J. Ewer, A.L. Flaxman, P.M. Folegatti, D.R. Owens, M. Voysey, P.K. Aley, B. Angus, G. Babbage, S. Belij-Rammerstorfer, L. Berry, S. Bibi, M. Bittaye, K. Cathie, H. Chappell, S. Charlton, P. Cicconi, E.A. Clutterbuck, R. Colin-Jones, C. Dold, K.R.W. Emary, S. Fedosyuk, M. Fuskova, D. Gbesemete, C. Green, B. Hallis, M.M. Hou, D. Jenkin, C.C.D. Joe, E.J. Kelly, S. Kerridge, A.M. Lawrie, A. Lelliott, M.N. Lwin, R. Makinson, N.G. Marchevsky, Y. Mujadidi, A.P.S. Munro, M. Pacurar, E. Plested, J. Rand, T. Rawlinson, S. Rhead, H. Robinson, A.J. Ritchie, A.L. Ross-Russell, S. Saich, N. Singh, C.C. Smith, M.D. Snape, R. Song, R. Tarrant, Y. Themistocleous, K.M. Thomas, T.L. Villafana, S.C. Warren, M.E.E. Watson, A.D. Douglas, A.V.S. Hill, T. Lambe, S.C. Gilbert, S.N. Faust, A.J. Pollard, C.V.T.G. Oxford, Safety and immunogenicity of ChAdOx1 nCoV-19 vaccine administered in a prime–boost regimen in young and old adults (COV002): a single-blind, randomised, controlled, phase 2/3 trial, Lancet 396 (10267) (2021) 1979–1993.

[6] N. Al Kaabi, Y. Zhang, S. Xia, Y. Yang, M.M. Al Qahtani, N. Abdulrazzaq, M. Al Nusair, M. Hassany, J.S. Jawad, J. Abdalla, S.E. Hussein, S.K. Al Mazrouei, M. Al Karam, X. Li, X. Yang, W. Wang, B. Lai, W. Chen, S. Huang, Q. Wang, T. Yang, Y. Liu, R. Ma, Z.M. Hussain, T. Khan, M. Saifuddin Fasihuddin, W. You, Z. Xie, Y. Zhao, Z. Jiang, G. Zhao, Y. Zhang, S. Mahmoud, I. ElTantawy, P. Xiao, A. Koshy, W.A. Zaher, H. Wang, K. Duan, A. Pan, X. Yang, Effect of 2 inactivated SARS-CoV-2 vaccines on symptomatic COVID-19 infection in adults: a randomized clinical trial, JAMA 326 (1) (2021) 35–45.

[7] V. Shinde, S. Bhikha, Z. Hoosain, M. Archary, Q. Bhorat, L. Fairlie, U. Lalloo, M.S.L. Masilela, D. Moodley, S. Hanley, L. Fouche, C. Louw, M. Tameris, N. Singh, A. Goga, K. Dheda, C. Grobbelaar, G. Kruger, N. Carrim-Ganey, V. Baillie, T. de Oliveira, A. Lombard Koen, J.J. Lombaard, R. Mngqibisa, A.a.E. Bhorat, G. Benadé, N. Lalloo, A. Pitsi, P.L. Vollgraaff, A. Luabeya, A. Esmail, F.G. Petrick, A. Oommen-Jose, S. Foulkes, K. Ahmed, A. Thombrayil, L. Fries, S. Cloney-Clark, M. Zhu, C. Bennett, G. Albert, E. Faust, J.S. Plested, A. Robertson, S. Neal, I. Cho, G.M. Glenn, F. Dubovsky, S.A. Madhi, Efficacy of NVX-CoV2373 COVID-19 vaccine against the B.1.351 variant, N. Engl. J. Med. 384 (20) (2021) 1899–1909.

[8] A. Wagner, J. Jasinska, E. Tomosel, C.C. Zielinski, U. Wiedermann, Absent antibody production following COVID19 vaccination with mRNA in patients under immunosuppressive treatments, Vaccine 39 (51) (2021) 7375–7378.

[9] P. Shenoy, S. Ahmed, A. Paul, S. Cherian, A. Vijayan, S.A. Babu, A. Sukumaran, Inactivated vaccines may not provide adequate protection in immunosuppressed patients with rheumatic diseases, Ann. Rheum. Dis. 81 (2) (2021) 295–296.

[10] S.M. Moghimi, Allergic reactions and anaphylaxis to LNP-based COVID-19 vaccines, Mol. Ther. 29 (3) (2021) 898–900.

[11] I. Hadj Hassine, COVID-19 vaccines and variants of concern: a review, Rev. Med. Virol. 32 (4) (2021) e2313.

[12] Y. Lustig, N. Zuckerman, I. Nemet, N. Atari, L. Kliker, G. Regev-Yochay, E. Sapir, O. Mor, S. Alroy-Preis, E. Mendelson, M. Mandelboim, Neutralising capacity against Delta (B.1.617.2) and other variants of concern following Comirnaty (BNT162b2, BioNTech/Pfizer) vaccination in health care workers, Israel, Euro Surveill. 26 (26) (2021) 2100557.

[13] Williams, S.V., A. Vusirikala, S.N. Ladhani, E. Fernandez Ruiz De Olano, N. Iyanger, F. Aiano, K. Stoker, G. Gopal Rao, L. John, B. Patel, N. Andrews, G. Dabrera, M. Ramsay, K.E. Brown, J. Lopez Bernal, and V. Saliba, An outbreak caused by the SARS-CoV-2 Delta (B.1.617.2) variant in a care home after partial vaccination with a single dose of the COVID-19 vaccine Vaxzevria, London, England, April 2021. 2021. 26(27): p. 2100626.

[14] M. Hoffmann, N. Krüger, S. Schulz, A. Cossmann, C. Rocha, A. Kempf, I. Nehlmeier, L. Graichen, A.S. Moldenhauer, M.S. Winkler, M. Lier, A. Dopfer-Jablonka, H.M. Jäck, G.M.N. Behrens, S. Pöhlmann, The Omicron variant is highly resistant against antibody-mediated neutralization: Implications for control of the COVID-19 pandemic, Cell 185 (3) (2021) e11.

[15] M. Hoffmann, H. Kleine-Weber, S. Schroeder, N. Krüger, T. Herrler, S. Erichsen, T.S. Schiergens, G. Herrler, N.H. Wu, A. Nitsche, M.A. Müller, C. Drosten, S. Pöhlmann, SARS-CoV-2 cell entry depends on ACE2 and TMPRSS2 and is blocked by a clinically proven protease inhibitor, Cell 181 (2) (2020) 271–280 .e8.

[16] M. Haschke, M. Schuster, M. Poglitsch, H. Loibner, M. Salzberg, M. Bruggisser, J. Penninger, S. Krähenbühl, Pharmacokinetics and pharmacodynamics of recombinant human angiotensin-converting enzyme 2 in healthy human subjects, Clin. Pharmacokinet. 52 (9) (2013) 783–792.

[17] Llewellyn-Davies, P. APEIRON's APN01 shows clinical benefits for severely ill COVID-19 patients in phase 2 trial. 12/03/, 2021, [press release]. Available from: https://www.apeiron-biologics.com/wp-content/uploads/20210312_PR_APN01-topline-data_ENG.pdf.

[18] A. Zoufaly, M. Poglitsch, J.H. Aberle, W. Hoepler, T. Seitz, M. Traugott, A. Grieb, E. Pawelka, H. Laferl, C. Wenisch, S. Neuhold, D. Haider, K. Stiasny, A. Bergthaler, E. Puchhammer-Stoeckl, A. Mirazimi, N. Montserrat, H. Zhang, A.S. Slutsky, J.M. Penninger, Human recombinant soluble ACE2 in severe COVID-19, Lancet Respir. Med. 8 (11) (2020) 1154–1158.

[19] Y. Liu, Y. Yang, C. Zhang, F. Huang, F. Wang, J. Yuan, Z. Wang, J. Li, J. Li, C. Feng, Z. Zhang, L. Wang, L. Peng, L. Chen, Y. Qin, D. Zhao, S. Tan, L. Yin, J. Xu, C. Zhou, C. Jiang, L. Liu, Clinical and biochemical indexes from 2019-nCoV infected patients linked to viral loads and lung injury, Sci. Chin. Life Sci. 63 (3) (2020) 364–374.

[20] I. Hamming, M. Cooper, B. Haagmans, N. Hooper, R. Korstanje, A. Osterhaus, W. Timens, A. Turner, G. Navis, H. van Goor, The emerging role of ACE2 in physiology and disease, J. Pathol. 212 (1) (2007) 1–11.

[21] C. Lei, K. Qian, T. Li, S. Zhang, W. Fu, M. Ding, S. Hu, Neutralization of SARS–CoV-2 spike pseudotyped virus by recombinant ACE2-Ig, Nat. Commun. 11 (1) (2020) 2070.

[22] T. Tada, C. Fan, J.S. Chen, R. Kaur, K.A. Stapleford, H. Gristick, B.M. Dcosta, C.B. Wilen, C.M. Nimigean, N.R. Landau, An ACE2 microbody containing a single immunoglobulin Fc domain is a potent inhibitor of SARS-CoV-2, Cell Rep. 33 (12) (2020) 108528.

[23] X. Miao, Y. Luo, X. Huang, S.M.Y. Lee, Z. Yuan, Y. Tang, L. Chen, C. Wang, F. Wu, Y. Xu, W. Jiang, W. Gao, X. Song, Y. Yan, T. Pang, C. Chen, Y. Zou, W. Fu, L. Wan, J. Gilbert-Jaramillo, M. Knight, T.K. Tan, P. Rijal, A. Townsend, J. Sun, X. Liu, W. James, A. Tsun, Y. Xu, A novel biparatopic hybrid antibody-ACE2 fusion that blocks SARS-CoV-2 infection: implications for therapy, MAbs 12 (1) (2020) 1804241.

[24] M.G. Wing, T. Moreau, J. Greenwood, R.M. Smith, G. Hale, J. Isaacs, H. Waldmann, P.J. Lachmann, A. Compston, Mechanism of first-dose cytokine-release syndrome by CAMPATH 1-H: involvement of CD16 (FcgammaRIII) and CD11a/CD18 (LFA-1) on NK cells, J. Clin. Invest. 98 (12) (1996) 2819–2826.

[25] D.W. Lee, R. Gardner, D.L. Porter, C.U. Louis, N. Ahmed, M. Jensen, S.A. Grupp, C.L. Mackall, Current concepts in the diagnosis and management of cytokine release syndrome, Blood 124 (2) (2014) 188–195.

[26] W.S. Lee, A.K. Wheatley, S.J. Kent, B.J. DeKosky, Antibody-dependent enhancement and SARS-CoV-2 vaccines and therapies, Nat. Microbiol. 5 (10) (2020) 1185–1191.

[27] T. Peters, in: All About Albumin : Biochemistry, Genetics, and Medical Applications, Academic Press, San Diego, 1996, p. 432.

[28] E.G. Schmidt, M.L. Hvam, F. Antunes, J. Cameron, D. Viuff, B. Andersen, N.N. Kristensen, K.A. Howard, Direct demonstration of a neonatal Fc receptor (FcRn)-driven endosomal sorting pathway for cellular recycling of albumin, J. Biol. Chem. 292 (32) (2017) 13312–13322.

[29] M.T. Larsen, M. Kuhlmann, M.L. Hvam, K.A. Howard, Albumin-based drug delivery: harnessing nature to cure disease, Mol. Cell. Ther. 4 (2016) 3.

[30] D. Pilati, K.A. Howard, Albumin-based drug designs for pharmacokinetic modulation, Expert Opin. Drug Metab. Toxicol. 16 (9) (2020) 783–795.

[31] J.T. Andersen, B. Dalhus, J. Cameron, M.B. Daba, A. Plumridge, L. Evans, S.O. Brennan, K.S. Gunnarsen, M. Bjoras, D. Sleep, I. Sandlie, Structure-based mutagenesis reveals the albumin-binding site of the neonatal Fc receptor, Nat. Commun. 3 (2012) 610.

[32] M. Bern, J. Nilsen, M. Ferrarese, K.M.K. Sand, T.T. Gjølberg, H.E. Lode, R.J. Davidson, R.M. Camire, E.S. Bækkevold, S. Foss, A. Grevys, B. Dalhus, J. Wilson, L.S. Høydahl, G.J. Christianson, D.C. Roopenian, T. Schlothauer, T.E. Michaelsen, M.C. Moe, S. Lombardi, M. Pinotti, I. Sandlie, A. Branchini, J.T. Andersen, An engineered human albumin enhances half-life and transmucosal delivery when fused to protein-based biologics, Sci. Transl. Med. 12 (565) (2020) eabb0580.

[33] J. Valero, L. Civit, D.M. Dupont, D. Selnihhin, L.S. Reinert, M. Idorn, B.A. Israels, A.M. Bednarz, C. Bus, B. Asbach, D. Peterhoff, F.S. Pedersen, V. Birkedal, R. Wagner, S.R. Paludan, J. Kjems, A serum-stable RNA aptamer specific for SARS–CoV-2 neutralizes viral entry, Proc. Natl Acad. Sci. 118 (50) (2021) e2112942118.

[34] D. Viuff, F. Antunes, L. Evans, J. Cameron, H. Dyrnesli, B. Thue Ravn, M. Stougaard, K. Thiam, B. Andersen, S. Kjaerulff, K.A. Howard, Generation of a double transgenic humanized neonatal Fc receptor (FcRn)/albumin mouse to study the pharmacokinetics of albumin-linked drugs, J. Control. Release 223 (2016) 22–30.

[35] M.T. Larsen, H. Rawsthorne, K.K. Schelde, F. Dagnæs-Hansen, J. Cameron, K.A. Howard, Cellular recycling-driven in vivo half-life extension using recombinant albumin fusions tuned for neonatal Fc receptor (FcRn) engagement, J. Control. Release 287 (2018) 132–141.

[36] K.Y. Huang, M.S. Lin, T.C. Kuo, C.L. Chen, C.C. Lin, Y.C. Chou, T.L. Chao, Y.H. Pang, H.C. Kao, R.S. Huang, S. Lin, S.Y. Chang, P.C. Yang, Humanized COVID-19 decoy antibody effectively blocks viral entry and prevents SARS-CoV-2 infection, EMBO Mol. Med. 13 (1) (2021) e12828.

[37] S. Tanaka, G. Nelson, C.A. Olson, O. Buzko, W. Higashide, A. Shin, M. Gonzalez, J. Taft, R. Patel, S. Buta, A. Richardson, D. Bogunovic, P. Spilman, K. Niazi, S. Rabizadeh, P. Soon-Shiong, An ACE2 triple decoy that neutralizes SARS–CoV-2 shows enhanced affinity for virus variants, Sci. Rep. 11 (1) (2021) 12740.

[38] Z. Zhang, E. Zeng, L. Zhang, W. Wang, Y. Jin, J. Sun, S. Huang, W. Yin, J. Dai, Z. Zhuang, Z. Chen, J. Sun, A. Zhu, F. Li, W. Cao, X. Li, Y. Shi, M. Gan, S. Zhang, P. Wei, J. Huang, N. Zhong, G. Zhong, J. Zhao, Y. Wang, W. Shao, J. Zhao, Potent prophylactic and therapeutic efficacy of recombinant human ACE2-Fc against SARS-CoV-2 infection in vivo, Cell Discov. 7 (1) (2021) 65.

[39] N. Eroshenko, T. Gill, M.K. Keaveney, G.M. Church, J.M. Trevejo, H. Rajaniemi, Implications of antibody-dependent enhancement of infection for SARS-CoV-2 countermeasures, Nat. Biotechnol. 38 (7) (2020) 789–791.

[40] O.A. Mandrup, S.C. Ong, S. Lykkemark, A. Dinesen, I. Rudnik-Jansen, N.F. Dagnæs-Hansen, J.T. Andersen, L. Alvarez-Vallina, K.A. Howard, Programmable half-life and anti-tumour effects of bispecific T-cell engager-albumin fusions with tuned FcRn affinity, Commun. Biol. 4 (1) (2021) 310.

[41] G. Ragia, V.G. Manolopoulos, Inhibition of SARS-CoV-2 entry through the ACE2/TMPRSS2 pathway: a promising approach for uncovering early COVID-19 drug therapies, Eur. J. Clin. Pharmacol. 76 (12) (2020) 1623–1630.

[42] R.B. Rosa, W.M. Dantas, J.C.F. do Nascimento, M.V. da Silva, R.N. de Oliveira, L.J. Pena, In vitro and in vivo models for studying SARS-CoV-2, the etiological agent responsible for COVID-19 pandemic, Viruses 13 (3) (2021).

[43] M.L. Yeung, J.L.L. Teng, L. Jia, C. Zhang, C. Huang, J.P. Cai, R. Zhou, K.H. Chan, H. Zhao, L. Zhu, K.L. Siu, S.Y. Fung, S. Yung, T.M. Chan, K.K.W. To, J.F.W. Chan, Z. Cai, S.K.P. Lau, Z. Chen, D.Y. Jin, P.C.Y. Woo, K.Y. Yuen, Soluble ACE2-mediated cell entry of SARS-CoV-2 via interaction with proteins related to the renin-angiotensin system, Cell 184 (8) (2021) 2212–2228 .e12.

[44] M. Donoghue, F. Hsieh, E. Baronas, K. Godbout, M. Gosselin, N. Stagliano, M. Donovan, B. Woolf, K. Robison, R. Jeyaseelan, R.E. Breitbart, S. Acton, A novel angiotensin-converting enzyme-related carboxypeptidase (ACE2) converts angiotensin I to angiotensin 1-9, Circ. Res. 87 (5) (2000) E1–E9.

[45] J. Nilsen, E. Trabjerg, A. Grevys, C. Azevedo, S.O. Brennan, M. Stensland, J. Wilson, K.M.K. Sand, M. Bern, B. Dalhus, D.C. Roopenian, I. Sandlie, K.D. Rand, J.T. Andersen, An intact C-terminal end of albumin is required for its long half-life in humans, Commun. Biol. 3 (1) (2020) 181.

[46] H.L. Zhao, X.Q. Yao, C. Xue, Y. Wang, X.H. Xiong, Z.M. Liu, Increasing the homogeneity, stability and activity of human serum albumin and interferon-alpha2b fusion protein by linker engineering, Protein Expr. Purif. 61 (1) (2008) 73–77.